Earth Reinforcement Practice, Ochiai, Hayashi & Otani (eds) © 1992 Balkema, Rotterdam. ISBN 90 5410 093 1

Bearing capacities and deformations of sand reinforced with geogrids

J.Takemura, M.Okamura, N.Suemasa & T.Kimura
Tokyo Institute of Technology, Japan

ABSTRACT: This paper describes the results of centrifuge model tests carried out to study the bearing capacities and failure mechanisms of sand reinforced with geogrids with high tensile strength. It is found that, just before the load intensity reaches its peak, a rigid soil block is formed under a footing irrespective of the replacement conditions and that this block behaves as if it were an embedded footing. At the peak the geogrid breaks and slip lines develops very rapidly, followed by a sharp decrease in the bearing capacities. The modes of failure after the peak are influenced by placement conditions of geogrids. The bearing capacities are similar even for the different conditions, where observed slip lines are similar.

1 INTRODUCTION

The bearing capacity and subgrade reaction of soil can be increased by reinforcement with geomaterials with high tensile strength and stiffness. Huang and Tatsuoka(1988) performed a series of model loading tests on sand reinforced with horizontal strips using a 10cm wide rigid strip footing. They reported that the failure modes could be classified into two types depending upon the density of the strips and proposed a method for calculating the bearing capacity for each failure mode. In order to evaluate the stability of soil against external loads properly, it is crucial to employ a reasonable failure mechanism. Since the mechanical behaviour of reinforced soil depends on many factors, such as the material properties of soils and of geogrids and the geometrical conditions of the placement of the reinforcement, it is extremely difficult to determine the correct failure mechanism.

Generally the tensile strength of geogrids is very high, therefore for the stability of slopes reinforced with geogrids the pullout capacity is more critical to the failure than the tensile strength of the grid itself. However, the pullout capacity in sand is roughly proportional to the normal stress on the surface of the grid, so in the areas where the stress becomes very high due to external load as in the areas near the footing the pullout resistance could be larger than the strength of the grid and the tensile rupture of the grid could be onset of the failure of the foundation. In other words the failure mechanism of the reinforced soil depends not only on the material properties of the grid as well as the placement conditions but also on the stress level in soil. In order to obtain reliable results from model tests on sandy soil reinforced with geogrids, it is essential to introduce the stresses similar to those in real life.

The authors have attempted to carry out a series of two-dimensional centrifuge model tests to study the bearing capacities of sand reinforced with geogrids having very high tensile strength. A special emphasis was placed on the observations of the failure mechanisms of reinforced soil under various conditions of placement.

2 TEST PROCEDURES

Model ground was made from dry Toyoura sand with index properties listed in Table 1. The geogrid used in the model test is FRP type grid which is made of continuous fiber glass formed with synthetic resin. The fiber has a very high stiffness of about 10GPa, nearly half of that for steel. The FRP type grid has a smaller failure strain and higher strength than the polymer type

Table 1 Physical properties of Toyoura sand.

Specific gravity	G_s	2.64
Mean diameter	D_{50} (mm)	0.19
Coefficient of uniformity	U_c	1.56
Maximum void ratio	e_{max}	0.973
Minimum void ratio	e_{min}	0.609

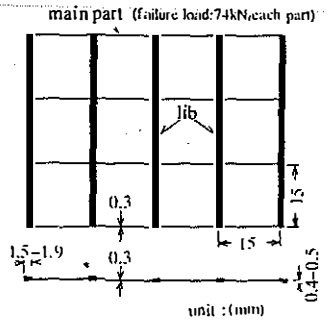

Fig.1 Model geogrid

Table 2 Test conditions.

Test code	Width of reinforcement W	Number of reinforcements N	Depth of placement (cm)	Settlement at end of loading s_f/B(%)
G35	3B	5	1,2,3,4,5	37
G35-1				12
G35-2				17
G35-3				17
G25	2B			36
G15	1B			39
G00	no reinforcement			34
G33	3B	3	1,3,5	38
G33-1				13
G34		4	1,2.3,3.7,5	38
G31		1	1	37
GR55	5B	5	1,2,3,4,5	39
GR00	no reinforcement			32

GR55,GR00: 1g tests

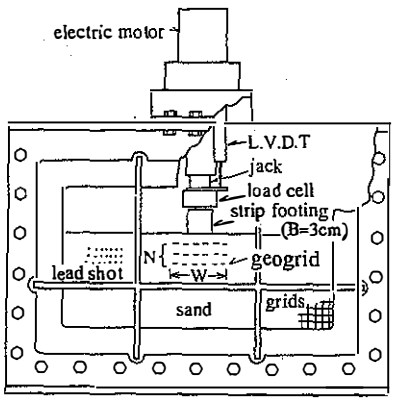

Fig.2 Test set-up.

grids. The model geogrid has a structure illustrated in Fig.1. The tensile strength is 7.8kN/m and the failure strain is 2.3%. Under 15g centrifugal acceleration employed for this model test the strength of corresponding prototype is 72kN/m and the stiffness is about 5 times higher than that for the polymer type grid.

The internal dimension of a centrifuge strong box is 500mm in length, 150mm in breadth and 350mm in height. Main parts of the box are made of steel except the front window which consists of a hard glass plate with stiffeners. Dry Toyoura sand was carefully rained down from a hopper into the box to form a sand layer with dry density of 1.6g/cm^3, of which thickness was 20cm. During this process, lead shots which are displacement markers were placed in every 1cm thickness and the model geogrids were installed horizontally at predetermined depths. In order to reduce the side-wall friction the surface of the inner wall was lubricated by placing 0.2mm thick rubber membrane smeared with silicone grease. On the surface of the membrane, 5mm-square grids were drawn for the observation of deformations of the ground during loading.

On completion of the model preparation, radiographs were taken to determine the initial locations of the lead shots buried in the ground. Having mounted the loading jack as shown in Fig.2, the strong box was placed in a centrifuge and the centrifugal acceleration was increased up to 15g. Loading tests were carried out using a rough footing with width(B) of 3cm, for various conditions of reinforcement; length(W), number(N) and spacing of the grid. The rate of loading was 1mm/min. After the test radiographs were again taken to read off the locations of the lead shots and to detect slip lines in the ground. Subsequently postmortem examinations were conducted to check the condition of the model grids.

Centrifuge tests in this study were divided into two groups. In the first group to study the effec of the width of reinforcement, three mode geogrids with the length of 1B, 2B and 3B were used and five of each grid were placed betwee the depth of 1cm and 5cm in 1cm spacing. I other group to study the effect of the spacing, 3 model grids were placed between the depth o 1cm and 5cm, changing the number of grid between 1 and 5. As a reference, sand with n reinforcement was also tested in 15g. The tes conditions are summarized in Table 2. The firs number of the test code denotes the W/B an second specifies N.

The loading test was continued until the footin settlement reached about 35% of the footin width. Additional tests for the cases o W=3B,N=5 and W=3B,N=3 were performed, i which loading was stopped at the peak load t see the progress of the failure, i.e.,slip lines an

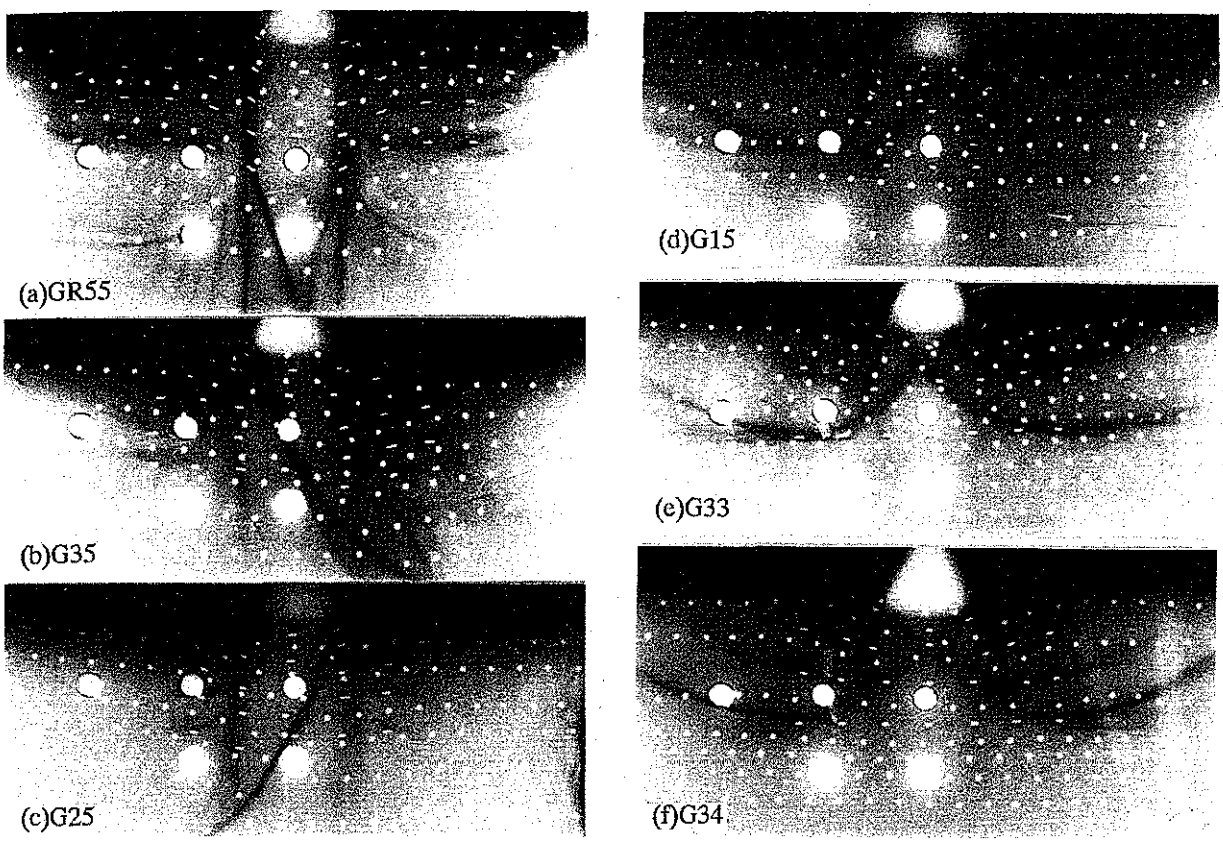

Fig.3 Radiographs of model ground subjected to large settlement (s/B=35%).

ruptures of the grids. In addition to these centrifuge tests, two gravity(1g field) model tests were conducted.

3 RESULTS AND DISCUSSIONS

3.1 Comparison of the gravity and centrifuge model tests

Fig.3 shows radiographs taken after the tests in which the footing was pushed into soil up to 35% of its width. Although in the gravity model test with W=5B and N=5:(a)GR55 no rupture was detected in any grid and the grids located outside the footing were pulled inwards, in the centrifuge model test with W=2B and N=5:(c)G25 the grids were ruptured. In the former case a soil block with a rectangular shape was observed, while in the latter a well-defined slip line extending from the edge of the footing to deep parts of the ground was noticed. This difference in the failure conditions of the grids and shapes of slip lines are considered to be due to the difference of the stress level in the ground. This implies that the failure mechanism of reinforced sand is influenced strongly by the size of footings.

3.2 Bearing capacities

Load intensity and settlement curves obtained from the loading tests are shown in Fig.4. In the figure load intensity:q and settlement:s were normalized by γB and B respectively. Repeatability of the test results can be confirmed from the curves for tests G35, G35-1,2 and 3, and G33 and G33-1 which have identical test conditions.

Reinforcement of sand with geogrids with high tensile strength is very effective both for increasing the bearing capacity q_f and the coefficient of subgrade reaction q_i/s_i. They increase with the increase in the width and the number of geogrid. Settlements at the peak load intensity also increase with the width and the number. The curves show a smooth increase up to the peak and a sharp decrease after the peak. This brittle behaviour must be taken into consideration in the determination of allowable bearing capacity. It is also interesting to see that residual bearing capacities are very similar for the cases of G25 and G35 and also for the cases of G15 and G00.

In Fig.5 the relationship between q_f and q_i/s_i are plotted against N and W respectively. It is seen

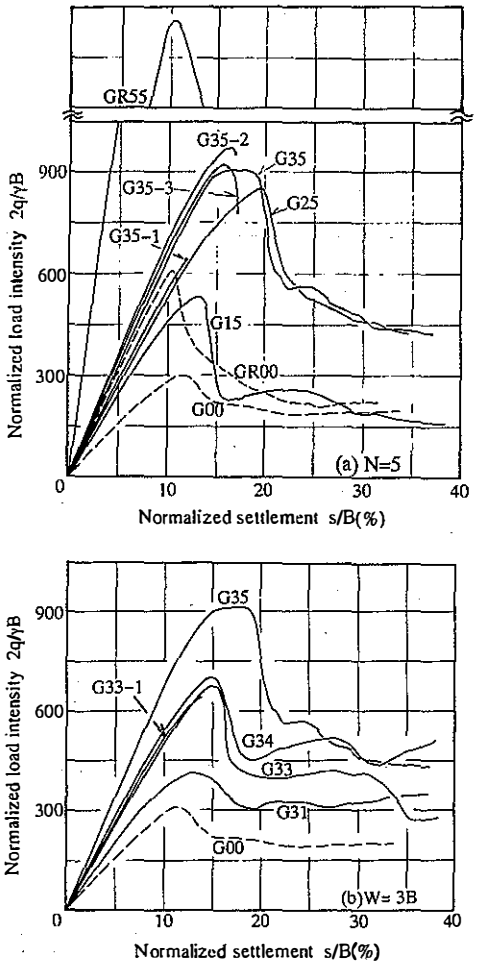

Fig.4 Normalized load intensity–settlement curves.

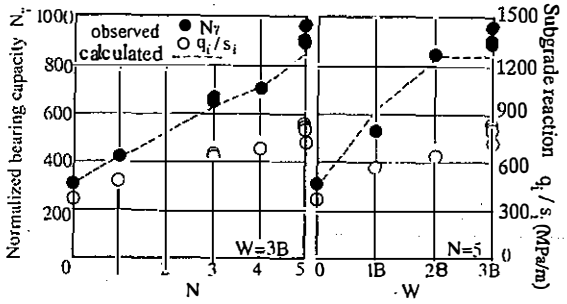

Fig.5 Normalized bearing capacity and subgrade reaction at initial portion of loading.

that the bearing capacity and the coefficient of subgrade reaction were increased by 300% and 250% respectively for five 3B grids placed in 1cm spacing. For the tests with W=3B, no substantial increase for both q_f and q_i/s_i can be noticed between N=3 and 4. This is also true for between N=2B and 3B for the tests with N=5. The bearing capacity of reinforced sand dose not increase linearly with W and N, but shows a complicate nature. Change in failure mechanism is considered to be responsible for this.

3.3 Deformation and failure mechanism

Contours of maximum shear strains at the end of loading are shown in Fig.6 together with the condition of geogrids. In the cases of G25 and G35 slip lines extended from a footing edge to deep parts which traverse all the geogrids were observed and the geogrids placed at deeper parts were ruptured. On the other hand, in other cases slip lines appeared in shallow parts above the deepest geogrid and the rupture of the deepest grid was not observed. Slip lines along the deepest grid were observed in the cases of G33 and G34. It can be concluded that the pattern of slip lines and positions of the rupture of geogrids are influenced significantly by the condition of the placement of geogrid. Especially for the cases of N=5, the change in the failure mechanism took place between W=B and W=2B. Comparing the bearing capacities shown in Fig.5 with the observed failure conditions in Fig.3, it can be said that bearing capacities for the cases where similar slip lines were observed are similar as for G33 and G34 and G25 and G35.

Radiographs for G35–1 and 2 are given in Fig.7. For G35–1 in which loading was stopped just before the peak load intensity, well–defined slip lines extending from both edges of the footing vertically downward were observed. A soil wedge was formed under a block of soil between these slip lines. As a result of this, the soil block behaved just as an embedded footing. For G35–2 where loading was continued up to a post peak stage, a well–defined slip line traversing the soil block under the footing was observed and the pattern of the slip lines was very similar to that for G35(Fig.3(b)) in which a large settlement was given. From these patterns of slip lines, it can be concluded that the slip line traversing the soil block under the footing were formed in a very short time at a stage where the peak load intensity approached the peak. A sharp decrease of the load intensity just after the peak may be because of this sudden development of the slip line, which is a unique behaviour of reinforced sand with high tensile geogrids. This cannot be observed in a sand without reinforcement for which a progressive failure is typical. In G35–1 the rupture of geogrids did not take place, while in G35–2 4th and 5th geogrids from the top were broken as shown in Fig.8. As long as the rupture of the grids does not occur, the soil block under the footing is subjected to

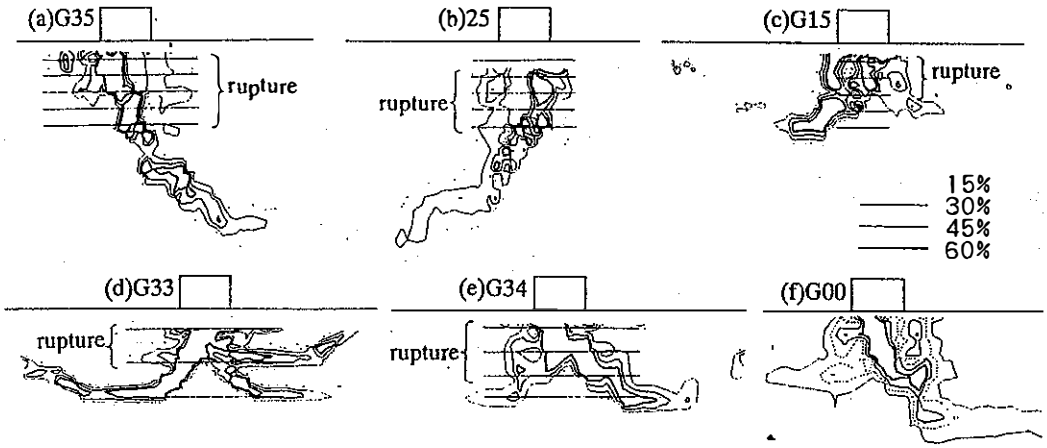

Fig.6 Contours of maximum shear strain and conditions of geogrid at the end of loading (s/B=35%).

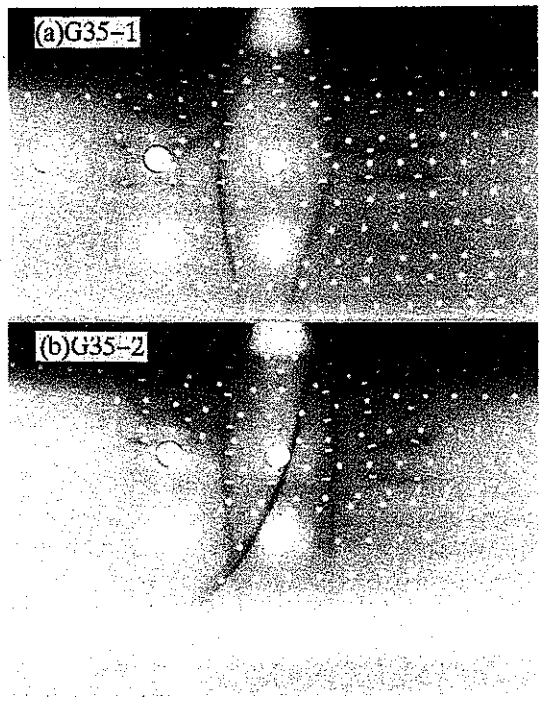

Fig.7 Radiographs taken just before and after peak load.

large confining stresses by the tension of the grids, resulting in very high shearing resistance. However, if one of the geogrids breaks, the confining stresses disappear causing a serious decrease of shearing resistance. This implies that the rupture of one grid triggers the development of slip lines traversing the soil block.

Binquet and Lee(1975a,b) carried out bearing capacity tests on reinforced sand with very long strips and reported that the strip in shallow parts broke first. The results of the test for W=3B and N=5 in this series are somewhat different; the grids embedded in deeper parts broke at first. One of the reasons for this may be that the pullout resistance turned out to be less than the strength of the grid in the author's test. It is considered that this was caused because the grid was too short to create enough pullout resistance at the shallow parts and the soil block underneath the footing took nearly all the load from the footing without distributing stresses to the parts outside the block, failing to increase the confining stresses.

Contours of the maximum shear strains at the peak load intensity, which were obtained from the photographs taken during the tests, are shown in Fig.9. Quantitative comparison is not possible because these contours are for different stages of the settlements. However, it can be seen that high sheared zones are developed from both edges of the footing, extending vertically downward, which compares well with the development of slip lines shown in Fig.7 for the case G35-1. The strains in the soil blocks between these zones are very small, again justifying consideration that these blocks are rigid. The depth of the sheared zones or the size of the soil block in the vertical direction increases with the number of geogrids.

4 BEARING CAPACITY CALCULATIONS

In this study an attempt was made to calculate the bearing capacity using Terzaghi's theory combining with an assumption that the soil block under the footing can be regarded as an embedment. The similar assumption was also adopted by Huang and Tatsuoka(1988). The bearing capacity can be given as

$$2q_f/\gamma B = N_\gamma + \frac{2D}{B} N_q \qquad (1)$$

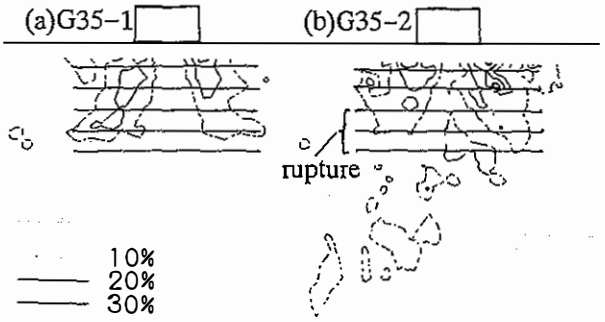

Fig.8 Contours of maximum shear strain and conditions of geogrid just before and after peak load.

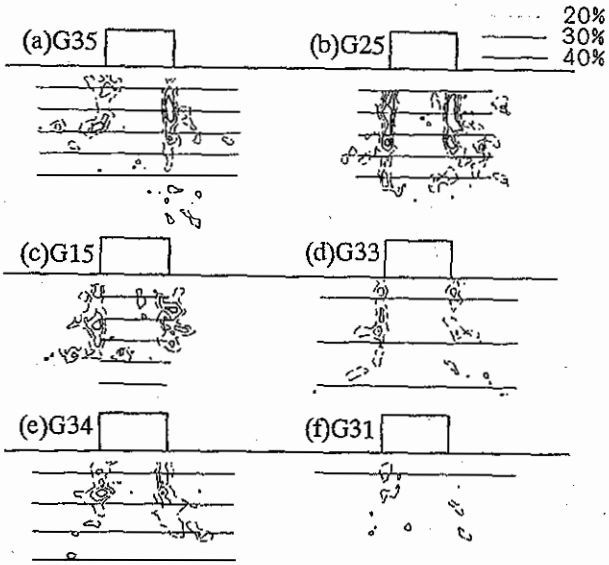

Fig.9 Contours of maximum shear strain at the peak load intensity.

where D is the imaginary depth of embedment. Friction angle ϕ', and other N_γ and N_q parameters were determined by back analyzing the observed bearing capacity for the test for unreinforced sand:G00 (N_γ=310), using Eq.(2) given by Vesic(1973) as

$$N_q = \frac{1+\sin\phi'}{1+\sin\phi'} \exp(\pi \tan\phi') \qquad (2)$$

$$N_\gamma = 2(N_q+1)\tan\phi'$$

The values obtained were ϕ=46°, N_γ=310 and N_q=160 respectively.

The results of the model tests show that the depth of highly sheared zones measured from the edges of the footing are 5cm for G25 and G35, 3.7cm for G34, 3cm for G33 and G15 and 1cm for G31. These depths were taken as imaginary depth of embedment D. The calculated bearing capacities are plotted against N and W in Fig.5, which compares well the observations. It can be said from this that the bearing capacities of soil reinforced with this type of grid can be estimated with reasonable accuracy if the imaginary depth of embedment can be determined properly.

5 CONCLUSIONS

Following conclusions were derived from this study on the bearing capacity of sand reinforced with geogrids with high tensile strength.

(1) Irrespective of the conditions as width and numbers of the geogrid, a rigid soil block is formed under a footing before the load intensity reaches its peak.

(2) At the peak one of the geogrids breaks and slip lines traversing the soil block develops in a very short time, followed by a sharp decrease in the bearing capacity.

(3) The pattern of slip lines and positions of the rupture of geogrids after the peak are influenced very much by the condition of the placement of geogrids. Especially, the change of the failure mechanism was observed between W=B and W=2B for the cases of N=5.

(4) Tests which produced similar slip lines give similar bearing capacities even for different conditions.

(5) The soil block under the footing behaves as if it were an embedded foundation; the deeper the block, the greater the bearing capacity. Bearing capacities estimated from Terzaghi's formula considering this effect of embedment compare well with the observed bearing capacities.

REFERENCES

Huang,C. & Tatsuoka,F.,1988, Prediction of bearing capacity in level sandy ground reinforced with strip reinforcement, International Geotechnical symposium on Theory and Practice of Earth Reinforcement, Fukuoka, pp.191-196.

Binquet,J. & Lee,K.L.,1975a, Bearing capacity tests on reinforced earth slabs, Proc. ASCE, Vol.101, No.GT12, pp.1241-1255.

Binquet,J. & Lee,K.L.,1975b, Bearing capacity analysis of reinforced earth slabs, Proc. ASCE, Vol.101, No.GT12, pp.1257-1276.

Vesic,A.S.,1973, Analysis of ultimate loads of shallow foundations, Proc. ASCE, Vol.99, No.SM1, pp.45-73.